Thermal and Optoelectrical analysis of $La_{0.7}Sr_{0.3}MnO_3$ Thin Film Thermistor in 8-12 µm range for Uncooled Microbolometer Application

Nirupam Paul
Dept. of Electrical Engineering
Indian Institute of Technology
Hyderabad, India
ee15resch02008@iith.ac.in

Sudharshan Vadnala
Dept. of Mechanical Engineering
Indian Institute of Technology
Bombay, India
ph10p005@iith.ac.in

Amit Agrawal
Dept. of Mechanical Engineering
Indian Institute of Technology
Bombay, India
amit.agrawal@iitb.ac.in

Siva R. Vanjari
Dept. of Electrical Engineering
Indian Institute of Technology
Hyderabad, India
svanjari@iith.ac.in

Shiv Govind Singh
Dept. of Electrical Engineering
Indian Institute of Technology
Hyderabad, India
sgsingh@iith.ac.in

***Abstract*—$La_{0.7}Sr_{0.3}MnO_3$ as a sensing material has shown an amazing potential for uncooled thermal imaging application. Here we report the fabrication of a $La_{0.7}Sr_{0.3}MnO_3$ (LSMO) thin film thermistor on a Si wafer and explored two prime figure-of-merit such as temperature coefficient of resistance (TCR) and optical responsivity, which are very useful parameters to compare the performance with any thermal sensor. The LSMO films were deposited on a $SrTiO_3$ (STO) buffer layer with Si/SiO_2 as a substrate, by a pulsed laser deposition (PLD) technique. The crystallinity and surface topography of the films were analyzed by X-ray diffraction (XRD) and atomic force microscopy (AFM). The fabricated device was then analyzed for its thermal and electrical characteristics to validate its suitability as an IR sensor. The fabricated device shows very sharp metal-to-insulator (T_{MI}) phase transition temperature at 150 K and very high TCR of +4% K^{-1} and -4%K^{-1} near 100 K and 200 K respectively, when the temperature was sweeped from 10 K to 300 K. Fabricated Thermistor shows very good thermal response and recovery when subjected to an alternating on-off cycle of IR lamp (150 W) illumination, which confirms its suitability for the high-speed thermal imaging application. The experimental analysis shows highest responsivity of ~21085 V/W at 8.5 µm, which falls in the Long-Wave Infrared (LWIR) region, which is an ideal IR band for any thermal imaging application.**

Keywords—LSMO, bolometer, TCR, thin film, responsivity.

I. INTRODUCTION

As a solution to the new industrial demand for better performance in the semiconductor industry, new functional oxides have been suggested for micro/nano device applications [1]. Typically known as rare-earth manganite oxides ($Re_{1-x}Ae_xMnO_3$, where Re is a rare earth element like La, Nd, Pr and Ae is an alkaline earth element, e.g. Ca, Sr, Ba, Pb), they normally have remarkable electronic and magnetic properties which are explored in several attractive device applications, such as in nonvolatile magnetic random access memories [2], magnetoresistive sensors and in spin electronic devices [3]. Moreover, manganites have a promising potential for bolometric infrared detection as these materials exhibit a significant change of their electrical resistance at the metal-to-insulator transition temperature (T_{MI}) when the temperature is varied over a wide range from 100-350 K [2, 4]. These materials undergo substantial change in their temperature coefficient of resistance (TCR, defined as TCR%= $\frac{1}{R}\frac{dR}{dT} \times 100$, where R and T represents the resistance and temperature) at the T_{MI} [5]. High TCR is one of the prerequisite electrical characteristic of an uncooled thermal detectors because it decides its sensitivity. Apart from that, high electrical conductance and low 1/f noise are some of the additional indispensable attributes of any superior class of material, considered ideal for IR sensing application [2].

In general, IR sensitive materials which are normally resistive in nature falls under two main categories namely metals (Au, Pt, Ti, etc.) [2] and semiconductors (VO_x, Amorphous silicon, SiGe,) [2, 6]. These materials are ideally supposed to have moderate to high TCR, high conductance, and low 1/f noise. When compared with other materials, manganites do exhibit relatively higher TCR near the transition (T_{MI}) temperature region, that determines the sensitivity as well as an active thermal zone for bolometer application. Indeed, the focus of our discussion is $La_{0.7}Sr_{0.3}MnO_3$ also known as LSMO which exhibits high TCR, high electrical conductance, and low noise [2]. In LSMO, the divalent Sr^{2+} ion doping at La^{3+} ion introduces extra holes in the valence band which enhance its electronic conductivity [7]. Furthermore, T_{MI} in LSMO can be tailored to a wide range of temperature by interstitial substitution technique which makes LSMO one of the potential sensing material for fabrication of uncooled thermal detectors [5]. In addition, stress/strain engineering in thin films also plays one of the key role to tune LSMO's phase transition temperature T_{MI} and TCR%. In literature, Goyal *et al.* reported +2 %K^{-1} TCR for 180 nm $La_{0.7}Sr_{0.3}MnO_3$ film on lanthanum aluminate (LAO) substrate at 360 K [8], Chaudhary *et al.* reported -7 %K^{-1} TCR for $La_{0.5}Sr_{0.5}MnO_3$ on Si substrate at 300 K [9], similarly Hayashi *et al.* reported TCR of +1.5%K^{-1} for 150 nm thickness of $La_{0.7}Sr_{0.3}MnO_3$ at 300 K on Strontium Titanate (STO) substrate [10], all of which signifies that the TCR value depends on various factors like film thickness, substrate type as well as the chemical composition of the film. Hence, LSMO has garnered a lot of interest among many researchers due to its wide range of options which it provides to fine tune the T_{MI} and TCR for the diverse bolometric application.

An uncooled infrared bolometer is a thermal detector whose electrical resistance changes as a function of radiant energy. So, the larger the resistance changes, it implies high TCR and high responsivity [11]. Infrared detectors are generally classified into two types: photon detectors and thermal detectors. The photon detectors have a high signal

978-1-5386-6415-5/18/$31.00 ©2018 IEEE

to noise ratio (SNR) and have a very fast response time, however, they generally require a cooling system, which makes them heavy, bulky and expensive. In comparison with photon detectors, most of the thermal detectors operate at room temperature, thus making them relatively economical and comparatively a bit noisy. Even though their response time is fairly large compared with the photon detectors, thermal detectors have no limitations on the wavelength response band. This makes it possible to used thermal detectors in hand-held infrared devices. Infrared detectors have diverse applications which are mainly used in temperature monitoring, thermal imaging, security, fire detection, search and rescue, and medical purposes.

In this study, $La_{0.7}Sr_{0.3}MnO_3$ thin film thermistor have been fabricated on a Si (100) wafer by pulsed laser deposition with $SrTiO_3$ as buffer layer sandwiched between LSMO and SiO_2. We have successfully shifted the transition temperature T_{MI} below the room temperature with very high TCR and responsivity values, which reiterates LSMO's enormous potential for infrared sensing. In addition, we have described the detailed fabrication of LSMO thin film thermistor and IR-based opto-electronic characterization of the fabricated device.

II. Device Fabrication and Thin Film Deposition

A. Device Fabrication

Fabrication of thin film thermistor to be used as a pixel in Microbolometer mainly involves fabrication of pixel structure, which is illustrated below in Fig. 1. The process starts with the drawing of the desired pixel pattern in CleWin software, as shown in Fig. 1(a) which will be printed on to the photomask. The pattern on the photo mask is then transferred to the photoresist (PR) (S1813) coated thermally oxidized P-type Si wafer during UV photolithography, which is illustrated in Fig. 1(b) and 1(c). The underlying SiO_2 layer which gets uncovered after developing the PR film was etched in buffered hydrofluoric (BHF) solution for about 5 to 6 minute, at room temperature condition with an observed etch rate of 100 nm/minute [12], unless the exposed SiO_2 is fully etched, as illustrated in Fig. 1(d).

The exposed Silicon was then etched using Reactive Ion Etching (RIE) system (NRE-3500) by $SF_6/CHF_3/O_2$ gas mixture at an optimized RF power of 150 W for 10 minutes as per the selected recipe, which has a physical etch rate of 1 µm/minute, as shown in Fig. 1(e). Fig. 1(f) shows the wafer after it is cleaned in Acetone and IPA bath for removal of PR and traces of acetone respectively, before dicing the wafer. Fig. 1(g) shows the schematic view of the device which was fabricated on the Si wafer. Hereafter the wafer is cleaved/diced into rectangular smaller pieces of suitable dimension (say 15 mm × 8 mm), the sample size which is suitable enough to be placed inside Pulsed Laser Deposition (PLD) chamber. The image of one of the sample is shown below in Fig. 2(a). Fig. 2 shows the diced SiO_2/Si sample which was used as a substrate during PLD process for LSMO film deposition and the probe station setup, Summit 11000 M from Cascade Microtech that was used for IR and electrical characterization.

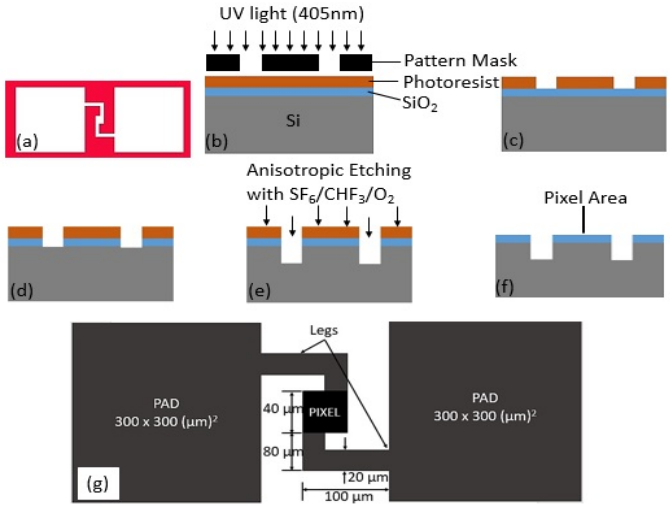

Fig. 1. (a) The mask pattern for fabricating the device, (b) Lithography step after spin coating, (c) when photoresist was developed after UV exposure, (d) after etching the SiO_2 layer in BHF solution, (e) etched profile after RIE etching, (f) pattern after stripping the photoresist film and (g) schematic of the etched device.

B. PLD Film Deposition Process

The PLD system uses Nd-YAG laser of 532 nm wavelength, having a pulse width and pulse energy of 8 ns and 300 mJ respectively, at 5 Hz for ablation. During the deposition, the pulsed laser was focused on a target, which is a circular pellet of 13 mm diameter and 3 mm in thickness. The target was rastered continuously during ablation, in order to avoid repeated ablation from the same spot on the target to ensure uniform erosion of the target material during the deposition process. The deposition of the film was carried out at 700 □ under high vacuum condition (5×10^{-5} mbar) and in a dynamic oxygen (O_2) pressure of 150 mTorr on a Si/SiO_2 substrate which is kept 45 mm away from the target. The substrate was mounted slightly off axis with respect to the plume axis and rotated at the rate of 8 rpm during the deposition in order to get a uniform film thickness. First Strontium Titanate (STO) buffer layer was deposited prior to LSMO film, primarily to reduce the strain in LSMO film which gets induced due to lattice mismatch with the substrate, if LSMO film was deposited directly on Si/SiO_2 substrate [13,14]. Approximately 500 and 6000 laser pulses were used for 10 nm and 175 nm thickness of STO and LSMO thin films respectively, the schematic view of which is shown in Fig. 3 below. For the deposited film, XRD technique (CuKα radiation) at 40 kV and 30 mA (PAN analytic X'pert pro) and AFM was used to analyze the structural morphology.

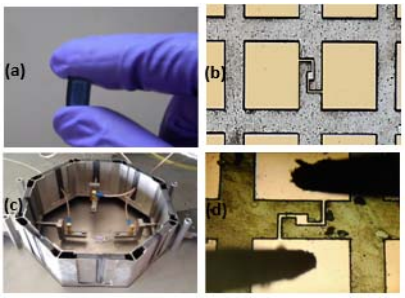

Fig. 2. Diced Silicon sample (a) sample used for PLD deposition, (b) Enlarged image of the fabricated device with Au/Ti contact pad, (c) the probe station setup with PLD sample, and (d) the single device when it was probed.

III. RESULTS AND DISCUSSION

A. Structural and Morphological characterization

Fig. 3(a) shows the GI-XRD pattern of LSMO thin film grown at 150 mTorr oxygen partial pressure along with the pattern of LSMO bulk ceramics. LSMO thin film exhibits polycrystalline structure with orthorhombic phase. It is very well matched with the bulk ceramic sample with PCPDF reference number 894461. Fig. 3(b) represents topography images of the LSMO thin film measured by Atomic force microscopy. It is observed that the thin film displays a smooth surface having its r.m.s surface roughness of less than 5 nm.

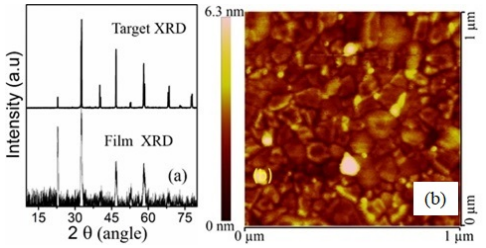

Fig. 3. (a) XRD analysis of LSMO thin film is compared with the ceramic bulk target, (b) Surface topography of LSMO thin film measured by atomic force microscope.

B. Electrical properties with IR illumination

In order to determine the suitability of any thin film for its sensing application, it becomes mandatory to study its electrical behaviour. Here we investigated the LSMO film for its sensitivity due to the heating effect of Infrared (IR) radiation, its TCR, temperature dependent I-V characteristics and its switching properties with alternating ON-OFF cycle of IR lamp exposure, to explore its overall suitability for IR sensing application. From this analysis, it is possible to extract many important performance parameters needed for characterizing the Optoelectrical behaviour of the film. We know that IR radiation causes heating effect which results in increase of temperature, therefore, we investigated the dependency of film resistance due to varying temperature by sweeping the temperature from 10K to 300K with a Closed Cycle helium refrigerator setup comprising of Keithley 6221 AC/DC current source and Keithley 2182A Nano voltmeter, for biasing the sample with a supply current of 10 mA and for measuring the voltage drop across the sample respectively. Fig. 4(a) illustrates the variation of film resistance with increasing temperature, using which it is possible to determine the two of the very important performance parameter like TCR and Responsivity of the thin film, which are needed for comparing their figure-of-merit with other sensors for use in IR sensing application. Interestingly, LSMO exhibits metal-to-insulator transition (T_{MI}) around 150 K. For $T < T_{MI,}$ the film behaves like a metal as its TCR is positive in that range and for $T > T_{MI}$ it behaves like a semiconductor, due to its negative TCR value. TCR is one of the figure-of-merit used to compare the performance of different materials for IR sensing application. The TCR of the film indicates the sensitivity of the film to an exposed IR. Higher the TCR value, higher will be the sensitivity of the material. During our measurement we observed TCR % varying from +4 %/K to -4.0 %/K (Fig. 4(b)) which is much higher than many results reported earlier [15-19].

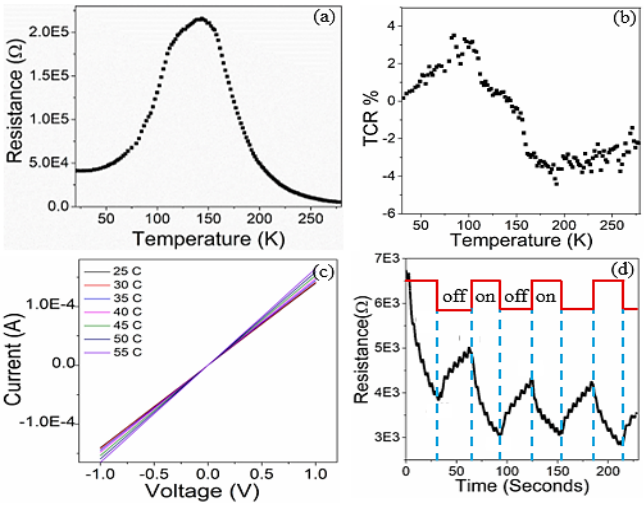

Fig.4. (a)The resistance vs temperature curve showing metal-to-semiconductor phase transition behaviour, (b) TCR % vs temperature curve, (c) I-V characteristics at different temperature and (d) switching response of thin film thermistor due to alternating cycle of IR lamp exposure for 30 secs with 50% duty cycle.

Fig. 4(c) shows the current-voltage (I-V) curves measured with a two-probe setup (Fig. 2(d), the schematic of which is shown in figure 5(a)) at normal atmospheric temperature and pressure. The characterization setup for two-probe measurement consists of a blackbody IR source (Model IR-2106 from Infrared Systems Development Corporation), for illuminating the sample, Keithley 4200 SCS Parameter Analyzer as Source Measuring Unit (SMU) and Probe Station (Model Summit 11000M from Cascade Microtech) for probing the sample. During I-V measurement the IR source temperature was varied uniformly from 25 □ to 55 □ in 5 □ step, and the respective I-V plot is shown in Fig. 4(c). All the curves for different temperature are perfectly linear and they are passing through the origin, which signifies that the film as-well-as contact point is perfectly ohmic in nature and it is behaving like a two-terminal resistor, obeying ohm's law. There is a gradual increase in the slope of the linear I-V curves as the temperature is increased uniformly, which illustrates thin film is semiconducting in nature. It is this characteristic which makes LSMO an ideal material for bolometer application.

The switching characteristics of the Thin film Thermistor was investigated using a series circuit consisting of the fabricated thermistor and a fixed resistor, which are approximately equal in resistance, and biased the circuit with a 1 V DC using an SMU, the circuit schematic for analyzing the switching characteristics is shown in figure 5(b). Fig. 4(d) shows the switching response when we illuminated the thin film sample with an IR lamp (150 W) by cyclically turning it on and off for 30 seconds with 50% on-off duty cycle. The periodical rise and fall of thin film resistance was captured using 16-channel AB4001 data acquisition system. Thermistor resistance starts falling very fast when illuminated with IR and it tends to increase when not exposed. But, we noted reduction in the peak value of resistance of the fabricated Thermistor in the subsequent off period during on-off cycle, due to high thermal capacitance of the substrate. As the experiment was performed in an open type environment with the thin film sample at normal atmospheric pressure condition, the effect

of stray noise due to various nearby electrical equipment and electromagnetic interfaces (EMI) could have caused those jitter in the switching response.

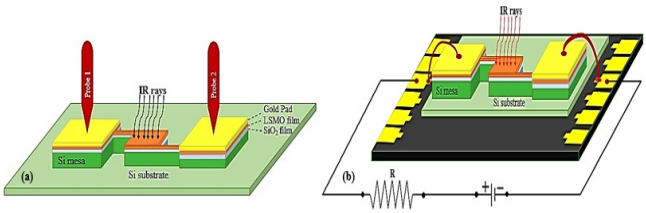

Fig. 5. (a) Schematic view of two-probe being used during I-V measurement, and (b) schematic view of the series circuit used for analyzing the switching response and optical responsivity.

Finally, we determined the responsivity of the LSMO film, which is used as one of the figure of merit to compare the performance with existing IR sensors. Responsivity is measured to determine the IR sensitivity, which primarily signifies the ability of the film to convert an incoming radiation into an electrical signal. As responsivity could be either voltage responsivity or current responsivity, it depends on whether we are measuring the voltage change or current during optoelectrical measurements. Here we used the same series circuit that was used for investigating the switching behaviour, for determining the voltage responsivity. The voltage responsivity is calculated by measuring the voltage change (ΔV) across the thin film due to the incident IR radiation and dividing it by the incident IR power, under fixed DC bias current.

$$R_v = \frac{\Delta V}{P_{in} \times A} = \frac{I_b \times \Delta R}{P_{in} \times A} \quad (1)$$

Where $\Delta V = V_{IR} - V_{dark}$ signifies change in output voltage when exposed with IR source, V_{IR} signifies the voltage developed during IR exposure, V_{dark} signifies the voltage in absence of any IR source. The incident power density of IR source (W/cm^2) is P_{in}, the sensing area of the sample (cm^2) is A, the DC bias current is I_b and finally the change in resistance caused by IR exposure is denoted by ΔR.The maximum responsivity obtained was 21085.6 V W^{-1}, which is very much higher than the values reported elsewhere previously [15] [20-26], when the bias current, change of resistance, incident IR power density and area are 6.4 µA, 1.5 KΩ, 29.328 mW cm^{-2} and 16 x 10^{-6} cm^2, respectively.

Fundamentally, the power density from IR source is related to its temperature by Plank's radiation law and the IR source temperature is dependent on the IR wavelength by Wein's displacement law. In Fig. 6 we have shown two graphs, the graph on the left side illustrates the dependency of responsivity on IR wavelength and the graph on the right side illustrates the dependency of IR source temperature on IR wavelength. The voltage responsivity was calculated for blackbody IR temperature range from 30 °C to 140 °C, at a fixed bias of 6.4 µA. Fig. 6 shows the variation of responsivity with IR wavelength, having a maximum value of 21085.6 V/W at 8.57 µm. It is to be noted that the respective IR wavelength of the temperature used during I-V measurement lies in the long wavelength IR range, as per the Wein's displacement law. Table I below clearly summarizes the superiority of LSMO thin film as IR sensitivity material with regards to TCR % and responsivity.

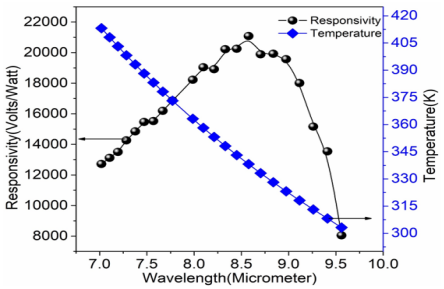

Fig. 6. Dependency of voltage responsivity as well as temperature on IR wavelength.

IV. CONCLUSION

In conclusion, we have illustrated the fabrication of a thin film thermistor followed by its material and IR-based optoelectrical characterization, to explore its suitability as an IR sensor. LSMO film deposited by a PLD process on STO buffered SiO_2/Si substrate, shows very good crystallinity and r.m.s surface roughness below 5 nm, as confirmed by XRD and AFM analysis respectively. TCR % of ±4%K^{-1} indicates LSMO films are highly sensitive and the reported result is much better than many results reported elsewhere. Temperature dependent I-V measurement shows linear curves passing through the origin with gradually increasing slopes as the temperature is varied uniformly in steps, which confirms the semiconducting nature of the LSMO film. Measured thin film resistance was in the range of 6 kΩ to 7 kΩ at room temperature, which reiterates the low noise nature of LSMO as IR sensing material. Good switching response and very high optical responsivity of~ 21085 V/W reaffirms that the fabricated LSMO thin film thermistor will be a better choice for the high speed thermal camera and it will be very much suitable for very long range thermal imaging application respectively, due to its higher sensitivity.

TABLE I. COMPARISON OF TCR AND RESPONSIVITY OF DIFFERENT IR SENSING MATERIAL

IR sensing material	Absolute TCR% (% K^{-1})	Responsivity (V/W)	Ref
Titanium	0.2	1.5	[20]
Aluminum	0.398	1050	[19]
CMOS N-well Layer	0.70	4970	[21]
Vanadium Pentoxide (V_2O_5) nanofibers	-1.6	6988.3	[16]
Poly SiGe	-2.0	47,800	[22]
Carbon Nanotubes (IsoNanotubes-S)	-2.1	138	[23]
Vanadium Oxide (VO_x)	-2.49	72000	[24]
Single-walled carbon nanotubes	-2.94	230	[25]
Vanadium-Tungsten alloy Oxide (VWO_x)	-2.98	5000	[26]
LSMO Thin Film	-4.0	21085.6	Current work

REFERENCES

[1] J.-H. Kim, A. M. Grishin, and V. A. Ignatova, "Wet Etching Study of $La_{0.67}(Sr_{0.5}Ca_{0.5})_{0.33}MnO_3$ Films on Silicon Substrates," in *Journal of Electron Materials,* vol. 37, no. 3, pp. 361–367, Mar. 2008.

[2] Ammar Aryan, Jean-Marc Routoure, Bruno Guillet, Pierre Langlois, Cédric Fur, Julien Gasnier, Carolina Adamo, Darrell Schlom, and Laurence Méchin, "Optical Characterization of La0.7Sr0.3MnO3 Thin Film Based Uncooled Bolometer," *SENSORDEVICES 2012, The Third International Conference on Sensor Device Technologies and Applications, Italy,* pp. 61-65, Aug. 2012.

[3] L. Méchin, J.M. Routoure, B. Guillet, F. Yang, S. Flament, D. Robbes, and R.A. Chakalov, "Uncooled bolometer response of a low noise $La_{2/3}Sr_{1/3}MnO_3$ thin film," *Appl. Phys. Lett.,* vol. 87 no. 20, p. 204103, Sep. 2005.

[4] Junmyung Lee, Jihun Kim, Min-Hee Hong, Hyung-Ho Park, Kwang-Ho Kwon, and Jaemin Lee, "Etching Characteristics and Mechanisms of LaSrMnO3 thin films inductively coupled plasmas as Halogen atoms for patterning of resistance layer in microbolometer," *The 6th International Conference on Microelectronics and Plasma Technology* (ICMAP)*,* Gyeongju, Korea (2016) 160190.

[5] J.-H. Kim, and A. M. Grishin, "Free-standing epitaxial La_{1-x} (Sr, Ca) $_xMnO_3$ membrane on Si for uncooled infrared microbolometer," *Appl. Phys. Lett.*, 87 (3) (2005) 33502.

[6] B. Guillet, L. Méchin, F. Yang, J.M. Routoure, G. Le Dem, C. Gunther, D. Robbes, and R.A. Chakalov, "Net of Ybco and Lsmo Thermometers for Bolometric Applications," in: *Advanced Experimental Methods for Noise Research in Nanoscale Electronic Devices,* Kluwer Academic Publisher, Netherland, pp. 327-336, (2004).

[7] M. Spankova, S. Chromik, I. Vavra, V. Strbík, J. Liday, P. Vogrincic, J. P. Espinos, and P. Lobotka, "Epitaxial LSMO films grown on GaAs substrates with MgO buffer layer," *Physica Status Solidi* (a) 206(7) (2009) pp. 1456-1460.

[8] A. Goyal, M. Rajeswari, R. Shreekala, S. E. Lofland, S. M. Bhagat, T. Boettcher, C. Kwon, Ramesh R., and T. Venkatesan, "Material characteristics of perovskite manganese oxide thin films for bolometric applications," *Applied physics letters*, 71(17) (1997) pp. 2535-2537.

[9] R. J. Choudhary, A. S. Ogale, S. R. Shinde, S. Hullavarad, S. B. Ogale, T. Venkatesan, R. N. Bathe, S. I. Patil, and R. Kumar, "Evaluation of manganite films on silicon for uncooled bolometric applications," *Applied physics letters* 84 (19) (2004) pp. 3846-3848.

[10] K. I. Hayashi, E. Ohta, and H. Wada, "Bi-Substitution Effect in La–Sr–Mn–O Thin Films for Bolometric Applications," *Japanese Journal of Applied Physics* 40(3A) (2001) L219.

[11] P. Lobotka, T. Lalinsky, M. Spankova, I. Vavra, S. Chromik, S. Hascik, V. Smatko, Z. Mozolova, E. Kovacova, J. Darer, and S. Gazi, "Antenna-coupled uncooled THz microbolometer based on micromachined GaAs and LSMO thin film," *Sensors*, 2008 IEEE, Lecce, Italy (2008) pp. 604-607.

[12] K. R. Williams, K. Gupta, and M. Wasilik, "Etch Rates for Micromachining Processing-Part II," *Journal of microelectromechanical systems* 12(6) (2003) pp. 761-778.

[13] R. R. Kumar, B. Karunagaran, D. Mangalaraj, S. K. Narayandass, P. Manoravi, M. Joseph, and V. Gopal, "Pulsed laser deposited vanadium oxide thin films for uncooled infrared detectors," *Sensors and Actuators A: Physical* 107(1) (2003) pp. 62-67.

[14] M. N. Ashfold, F. Claeyssens, G. M. Fuge, and S. J. Henley, "Pulsed laser ablation and deposition of thin films," *Chemical Society Reviews* 33(1) (2004) pp. 23-31.

[15] S. Vadnala, N. Paul, A. Agrawal, and S. G. Singh, "Enhanced infrared sensing properties of vanadium pentoxide nanofibers for bolometer application," *Materials Science in Semiconductor Processing* 81 (2018) pp. 82-88.

[16] H. K. Lee, J. B. Yoon, E. Yoon, S. B. Ju, Y. J. Yong, W. Lee, and S. G. Kim, "A high fill-factor infrared bolometer using micromachined multilevel electrothermal structures," *IEEE Transactions on electron devices* 46(7) (1999) pp. 1489-1491.

[17] M. Kolahdouz, A. A. Farniya, M. Östling, and H. H. Radamson, "The performance improvement evaluation for SiGe-based IR detectors," *Solid-State Electronics* 62(1) (2011) pp. 72-76.

[18] P. Eriksson, J. Y. Andersson, and G. Stemme, "Thermal characterization of surface-micromachined silicon nitride membranes for thermal infrared detectors," *Journal of Microelectromechanical systems* 6(1) (1997) pp. 55-61.

[19] N. Shen, J. Yu, and Z. Tang, "An Uncooled Infrared Microbolometer Array for Low-Cost Applications," *IEEE Photonics Technology Letters* 27(12) (2015) pp.1247-1249.

[20] W.-B. Song, and J.J. Talghader, "Design and characterization of adaptive microbolometers," *Journal of Micromechanics and Microengineering* 16 (5) (2006) pp. 1073-1079.

[21] S. Eminoglu, M. Y. Tanrikulu, and T. Akin, "A Low-Cost 128 × 128 Uncooled Infrared Detector Array in CMOS Process," *Journal of Microelectromechanical Systems* 17(1) (2008) pp. 20-30.

[22] S. Sedky, P. Fiorini, K. Baert, L. Hermans, and R. Mertens, "Characterization and optimization of infrared poly SiGe bolometers," *IEEE Transactions on Electron Devices* 46(4) (1999) pp. 675-82.

[23] K. Narita, R. Kuribayashi, E. Altintas, H. Someya, K. Tsuda, K. Ohashi, T. Tabuchi, S. Okubo, M. Imazato, and S. Komatsubara, "A plastic-based bolometer array sensor using carbon nanotubes for low-cost infrared imaging devices," *Sensors and Actuators A: Physica* 195 (2013) pp. 142-147.

[24] J. Grant, I. Escorcia□Carranza, C. Li, I. J. McCrindle, J. Gough, and D. R. Cumming, "A monolithic resonant terahertz sensor element comprising a metamaterial absorber and micro□bolometer," *Laser & Photonics Reviews* 7(6) (2013) pp. 1043-1048.

[25] G. Vera-Reveles, T. J. Simmons, M. Bravo-Sánchez, M. A. Vidal, H. Navarro-Contreras, and F. J. González, "High-sensitivity bolometers from self-oriented single-walled carbon nanotube composites," *ACS applied materials & interfaces* 3(8) (2011) pp. 3200-3204.

[26] N. Chi-Anh, H. J. Shin, K. Kim, Y. H. Han, and S. Moon, "Characterization of uncooled bolometer with a vanadium tungsten oxide infrared active layer," *Sensors and Actuators A: Physical* 123 (2005) pp. 87-91.